

BIOCHE 01807

Time-resolved fluorescence fractal analysis in lipid aggregates

Panagiotis Lianos^a and Guy Duportail^b

^a University of Patras, School of Engineering, Physics Section, 26500 Patras (Greece)

^b Centre des Recherches Pharmaceutiques, Laboratoire de Physique, UA CNRS 491: Université Louis Pasteur, B.P. 24, 67401 Illkirch Cedex (France)

(Received 14 February 1993; accepted in revised form 24 August 1993)

Abstract

A model called the "Percolation Model" is described which is successfully used to study bimolecular diffusion-controlled reactions in lipid aggregates. A time-dependent kinetic rate is calculated through this model and can be used to give information on several types of biological supramolecular assemblies. As an example, we present a time-correlated analysis of pyrene decanoate self-quenching by excimer formation in egg yolk phosphatidylethanolamine at its lamellar and hexagonal H_{II} phases.

Keywords: Time-resolved fluorescence; Fractal analysis; Lipid aggregates; Percolation model

1. Introduction and theory

For more than twenty years, time-resolved fluorescence probing has been used as a valuable tool to study both structure and dynamics of microheterogeneous systems such as micelles, microemulsions, lipid vesicles and polymers. In the vast majority of cases, it involves either analysis of the time dependence of fluorescence anisotropy or of the kinetics of a bimolecular reaction between a fluorescing minority species and a quenching majority species. Different models have then been used to interpret the fluorescence decay profiles. Thus, in the case of micelles and microemulsions, the quenching reaction is best described by the interaction between compartmentalized reactants, which are distributed among the available micelles [1–3]. Such a model cannot be extended to lipid vesicles or, in general, to biological supramolecular assemblies,

which are large and fairly complex systems. There have been several approaches to treat the fluorescence quenching reaction in lipid membranes. Vanderkooi and collaborators [4,5] considered the lipid vesicles above the gel-to-liquid crystal transition temperature as a viscous homogeneous liquid. They then interpreted the fluorescence decay profiles of pyrene monomers in the presence of excimers by a model based on the Einstein–Smoluchowski diffusion theory [6], according to which the reaction rate is time-dependent. However, Liu et al. [7] found that the fluorescence decay could be adequately described by a sum of three exponential terms and not by the above diffusion model. These authors suggested that the observed decay is compatible with a reaction scheme involving excited-state interactions. Later, Daems et al. [8] showed that above the phase transition temperature, the fluorescence decay of pyrene monomer could be fitted by either a sum

of exponentials or by the diffusion model while below the phase transition temperature only the diffusion model could fit the obtained data. By using pyrene-labelled phospholipids, Lemmetyinen et al. [9] proposed for the excimer formation process in the gel phase, a scheme involving two separate paths. The first one is a diffusion-controlled process and the second one is a static process where the pyrene moieties are aggregated in such a manner that a small motion suffices to attain excimer formation. The problem of probe aggregation has also been studied by authors using only steady-state fluorescence probing [10]. Recently, Pansu et al. [11] analyzed the mechanism of pyrene excimer formation using synthetic membranes, both in the gel and the liquid crystalline phase. These authors showed that in the rigid phase of the bilayers, a fraction of the probes is isolated and not submitted to reaction. This fraction was estimated with good precision by convolution analysis using transient-diffusion models. Finally, it is true that any fluorescence decay profile can be fitted by a sum of several exponential terms. However, in principle, an infinite number of exponential terms is necessary to ideally describe a decay profile. This requires, on the one hand, powerful computers which are not available to all laboratories and, on the other hand, there exists a large correlation between different exponentials, making the analysis uncertain. The problem of correlated exponentials recently has been solved by applying constraints, as in the so-called Maximum Entropy method [12]. We thus see that there has been an uncertainty as to the proper choice of a decay model capable of describing reactions in lipid vesicles in a uniform manner. We believe that this difficulty stems from the fact that all models used so far do not involve the notion of dimensionality. However, microheterogeneous phases are essentially systems of restricted geometry. For this reason, models describing reactions in such media must include a parameter related to the dimensionality of the reaction domain.

The most fundamental quantity necessary to describe the kinetics of a chemical reaction is the rate constant. Experimentally, another approach is followed in that the evolution of the monitored

reacting species is expressed versus time from which with the help of a kinetic model the rate constant is calculated. In cases of fluorescence probing, where an excited fluorophore is quenched by a quencher, the evolution of the reaction is monitored by fluorescence. Analysis then of the fluorescence decay profile gives the quenching rate constant. However, nowadays it is well understood that constant rates apply to only a part of the known kinetics, while spatial or energetic disorder leads to time-dependent rates. This is the case for fluorescence quenching in lipid aggregates which consist of microdomains, so therefore they possess geometrical disorder.

Fluorescence quenching in fluid media can be generally analyzed into two parts. One part is energy exchange between the excited and the quenching species. Energy can be transferred to a distance r by dipole or multipole interactions with probability obeying a power law $1/r^s$, where $s = 6, 8, 10$, etc., for dipole–dipole, dipole–quadrupole, quadrupole–quadrupole, etc., interactions, respectively [13,14]. Also energy can be transferred by electron transfer with probability proportional to $\exp(-kr)$, where k is a constant. In most of the cases, in particular in the cases which interest us here, the employed fluorescence quenching couples are such that no important transfer occurs when they are immobilized. The probability of a transfer can then be satisfactorily represented by a power law with large s values. The second part of fluorescence quenching in fluid media is a diffusion-controlled process. Allinger and Blumen [15] have derived a general equation for reactions occurring by both energy transfer and diffusion, using a power law for the transfer probability. Thus the survival probability of the decaying fluorescent species, represented by the time-dependent fluorescence intensity $I(t)$ is given (in a simplified form) by

$$I(t) \approx \exp \left[-At^{\Delta/s} + \sum_{n=1}^{\infty} B_n D^n t^{n-2n/s+\Delta/s} \right] \quad (1)$$

where Δ is the dimensionality of the reaction domain, D is the mutual diffusion coefficient and A and B are constants depending on Δ and the

occupation probability p of the available solubilization sites by quenchers (assuming that quenchers are much more numerous than excited fluorophores). Analytical expressions for B_n are given in ref. [15]. This equation, which is derived by ensemble averaging over all quenching possibilities, clearly separates the two parts of the interaction. Note that if Δ/s is a small number, as for the case of multipole interactions, then $At^{\Delta/s}$ corresponds to a very fast decaying contribution. This practically means that long-range transfer is negligible. Only very close together lying reactants can interact. Since reactants can come close by diffusion, only the diffusion-controlled part of the interaction, i.e. the infinite series of eq. (1), is of importance. On the other hand, for immobile reactants ($D = 0$), the only contribution is the energy transfer term $At^{\Delta/s}$.

Diffusion-controlled reactions in media with geometrical restrictions should then be modelled by the infinite series of eq. (1). On these reactions we further shall focus attention now, since most fluorescence quenching reactions in lipid vesicles are controlled by diffusion. Handling this infinite series is not an easy task. This problem has been solved in a very elegant way by Blumen, Klafter and Zumofen [16–18] by using ideas from the theory of fractal objects and the theory of random walks in fractal domains. Their work was formulated to apply to energy migration in solid media of spatial disorder. However, the same formulation applies also to diffusion-controlled bimolecular reactions between a minority and a majority species (dilute solution), if diffusion is modelled by a (mutual) random walk. We briefly present the basic theory leading to the derivation of the final form of the decay model. If reactants are considered as the random walkers, then the rate of reaction in a restricted environment depends on the number $S(t)$ of distinct sites visited by a random walker within a time t . Alternatively, we can say that a reaction is slow when a random walker visits and revisits the same sites before encountering a co-reactant. Thus $S(t) \approx t^f$, where $f < 1$, in a restricted environment and $S(t) \approx t$ in a homogeneous, non-viscous environment. Smaller f values correspond to more restricted environments. If the reaction domain is self-similar,

i.e. it is fractal, then f is related with the so-called spectral dimension d_s : $f = d_s/2$ where $d_s = 2d_f/d_w$, d_f is the fractal dimension and d_w the fractal dimension of the random walk [19]. By using a Sierpinski gasket as a model fractal and by making a cumulative expansion, Klafter and Blumen [18] have derived the following decay equation:

$$I(t) \approx \exp(-\lambda S(t) + \lambda^2 \sigma^2(t)/2 \dots) \quad (2)$$

This equation was shaped to apply to energy migration such that the same reasoning is applied for molecular migration (diffusion). In eq. (2), $S(t)$ is the number of distinct sites visited within a time t , as already said, while $\sigma^2(t)$ is its variance, i.e. $\sigma^2(t) = \langle S^2(t) \rangle - \langle S(t) \rangle^2$. $S(t) \approx t^f$ and $\sigma^2(t) \approx t^{2f}$ [12]. $\lambda = -\ln(1-p)$, where p is the occupation probability of sites by reactants, i.e., in our case, it is related with the number of the solubilization sites in the lipidic phase and the total reactant concentration. We might then rewrite eq. (2) in a more simplified form as

$$I(t) \approx \exp(-C_1 t^f + C_2 t^{2f} \dots) \quad (2a)$$

where C_1 and C_2 are constants. By comparison with eq. (2), it is obvious that C_1 and C_2 depend on reactant concentration but are not related through some simple mathematical relation. This is because C_1 is also proportional to $S(t)$ while C_2 is proportional to $\sigma^2(t)$, which reflect the particularities of the reaction domain itself. Obviously, eq. (2) is equivalent to the infinite series of eq. (1), i.e. it applies well to diffusion-controlled reactions. Note that eq. (2) as well as eq. (1) describe a specific dependence on both the geometry of the environment and the occupation probability. The reaction rate $K(t)$ is then easily derived from eq. (2) by differentiation [20]

$$K(t) = fC_1 t^{f-1} - 2fC_2 t^{2f-1} + \dots \quad (3)$$

This expression gives a first-order rate which, of course, is time-dependent, as expected.

We have shown that the fluorescence decay profile and the rate constant for diffusion-controlled quenching in a geometrically disordered medium should be expressed as an infinite series of terms containing non-integer powers of time.

In practical applications, two terms [20] suffice to fit an experimental decay profile but only one term is not always enough. In fact, it has been experimentally shown, by using reverse micelles, that the importance of the second term depends on the occupation probability, the geometry and also the lifetime of the monitored fluorescent species [21].

In order that a microheterogeneous system is represented by fractals it should possess the property of self-similarity. It is true that perfect fractals can be produced only on a computer screen, but any disordered system may show a lower or higher degree of self similarity, i.e. symmetry by dilatation, and such an assumption is amenable to confirmation by experiment.

The analysis of the fluorescence decay profiles with the help of stretched exponentials allows the calculation of the reaction rate as a function of time [20]. This is the great advantage of the present method. It allows us to monitor the reaction all along its evolution giving a fairly complete representation of the system and its dynamics. This quality is further stressed when reactants acting at different time scales are used [21,22]. Even more, it allows the detection of extremely fast kinetic processes which are found in cases of ground state complex formation and, generally, in stationary (or quasi-stationary) quenching [20,22]. In such cases the calculated f values are very small.

The model of eq. (2) has been applied in several studies of phospholipid vesicles to their gel, liquid-crystalline and hexagonal phases [20,22–26]. The actual equation used was:

$$I(t) = I_0 \exp(-k_0 t) \exp(-C_1 t^f + C_2 t^{2f}) \quad (4)$$

where k_0 is the decay rate in the absence of quenching. Our conclusions have been supported by computer simulations [27,28]. For computer simulations, we have used techniques previously reported [29]. Briefly, lattice clusters are generated and two reactants, A and B ($[A] \ll [B]$), are introduced into the clusters. Reaction proceeds by random walk within the clusters with the stipulation that if A and B occupy the same site they annihilate and are removed from the system while

nothing happens between two A and two B particles. The clusters, which constitute the dispersed phase, can be chosen to have random sizes. If the percentage of the dispersed phase is high enough (i.e. 59.3% for a two-dimensional and 31.2% for a three-dimensional lattice) then among the clusters formed one cluster extends from one side of the lattice to the other while the rest are smaller non-communicating clusters. Below the above threshold values, all clusters are non-communicating ones. In all cases we have a “percolation” pattern, either below or above the threshold. Thus the case of vesicles corresponds to a system below the percolation threshold. We have adopted the name “percolation model” for the present model. When applied to lipid vesicles the system behaves in the same manner as in lattice clusters below the percolation threshold.

2. Experimental results

As an application of the above theory, we present a time-correlated analysis of pyrene decanoate (PD) excimer formation in two structural phases of egg yolk phosphatidylethanolamine (EYPE), namely, the lamellar L_α and the hexagonal H_{II} phase. The results presented here are published for the first time.

Under certain conditions (e.g. low pH), unsaturated phosphatidylethanolamines (PEs) prefer non-bilayer structures, such as the inverted hexagonal phase (H_{II}). This non-bilayer structure is considered to be an intermediate state of membrane fusion while the transition from a bilayer to an hexagonal structure possibly modulates membrane functions, such as protein incorporation and activity. This property of PE has led to the proposition that PE may play an important role in controlling fusion through the destabilization of the bilayer [30,31]. In this work, we have studied the pH-induced hexagonal phase for EYPE multilamellar vesicles. At pH 9.5, this phospholipid forms vesicles in a L_α liquid crystalline bilayer phase. At pH 5.0, these vesicles undergo a $L_\alpha \rightarrow H_{II}$ phase transition around 25–35°C [32]. This transition can be detected by following the increase of the fluorescence of *N*-(7-nitro-2,1,3-

benzoxadiazol-4-yl) phosphatidylethanolamine (NBD-PE) labelling the vesicles at 1% ratio [33,34]. Thus, in Fig. 1 we can see the increase at 40°C of the fluorescence of EYPE multilamellar vesicles labelled with NBD-PE, from pH 9.5 to 5.0, which verifies the appearance of the H_{II} hexagonal phase.

EYPE multilamellar vesicles, containing PD at various ratios or 1% NBD-PE, were prepared by first mixing the phospholipid and the probe in a mixed chloroform-methanol (9:1) solution. The solvent was rotary evaporated under vacuum. After addition of an appropriate volume of pH 9.5 buffer (5 mM borate, 150 mM NaCl, 0.1 mM EDTA) such that the final concentration in phospholipids was always 2×10^{-4} M, the samples were vigorously vortexed for 2 min. The concentration of PD was checked by absorption spectrophotometry and was found to be quantitative at each ratio. Small quantities (a few μ M) of a concentrated (1 M) citric acid was used to lower the pH at 5.0.

All fluorescence decay data were registered at 40°C with non-deoxygenated samples by using the photon-counting technique. The excitation wavelength was 325 nm and the emission 385 nm (monomer PD emission). The fluorescence decay profiles were analysed with the help of eq. (4), convoluted with the excitation profile, as in ref. [25]. The first-order decay rate $K(t)$ was calculated with the help of eq. (3) while the second-order rate $k(t)$ was calculated by dividing $K(t)$ by the quencher (unexcited PD) concentration. The decay rate of PD in the absence of excimers was calculated at PD concentration equal to 10^{-6} M.

Table 1 shows the obtained results. The second column shows the values of the non-integer exponent f which is a measure of the restrictions of the lipid environment, as sensed by the diffusing PD molecules. Smaller f correspond to more restrictive environments. The diffusion-controlled reaction is more restricted when f is small, i.e. the reaction is then more localized. Our experience with reactions in lipid vesicles suggests that the values of f obtained here are rather large. This is due to the increased temperature and to the fact that the L_α phase is fairly fluid, easily

Table 1

Time-correlated analysis data obtained with pyrene decanoate at various concentrations in 2×10^{-4} M EYPE at pH 9.5 and 5.0 ($T = 40^\circ\text{C}$)

[PD] (10^{-6} M)	f	10^3 C_2/C_1	K_1, K_L (10^6 s $^{-1}$)	K_{AV}	k_1, k_L (10^{11} s $^{-1}$)	k_{AV} (M^{-1})		
<i>pH 9.5, $\tau_0 = 91.2$ ns</i>								
10	0.85	1.2	21	6.6	9.0	21	6.6	9.0
20	0.88	2.4	37	8.2	15	19	4.1	7.5
30	0.83	5.2	74	7.6	17	25	2.6	5.8
40	0.85	7.0	115	5.4	19	29	1.3	4.7
<i>pH 5.0, $\tau_0 = 82.0$ ns</i>								
10	0.85	1.7	32	8.8	13	32	8.8	13
20	0.85	2.3	57	9.0	21	29	4.5	10
30	0.85	4.0	103	6.6	29	34	2.2	9.5
40	0.84	6.3	143	0.0	24	36	0	6.0

permitting diffusion. Indeed, we have previously found [25] that f values change from 0.38 to 0.66 when dipalmitoylphosphatidylglycerol vesicles undergo a gel to liquid crystalline transition under temperature increase. As a consequence it is expected that this fluid environment would not be susceptible to important changes that would influence the f values upon transition to the H_{II} phase. Indeed f is found practically the same in the two phases.

The third column shows the values of the ratio C_2/C_1 (see eq. (4)) which is a measure of the importance of the second order approximation in fitting eq. (4) to the experimental decay profile. This ratio is large when f is small, when the quencher concentration is relatively large and when the decay time of the fluorophore is relatively small [21]. Our experience shows that the values found here are relatively small (cf. ref.[25]). This is partly due to the relatively large f values. However, these small values mainly suggest that in the present two phases of EYPE, there is a large number of possibilities for the solubilization of PD molecules. Thus the number of PD molecules is relatively small compared with the number of the available solubilization sites [21]. Nevertheless, it is not negligible, as seen by the increase of the C_2/C_1 ratio with PD concentration. Since the recorded fluorescence decay profile is an average, reflecting all the fluorescence quenching (i.e. diffusion-controlled excimer for-

mation) possibilities, we might alternatively say that the low C_2/C_1 values show that for the present system, the dispersion around the average value is small. As in the case of f , C_2/C_1 was not affected by the phase transition.

The next three columns show values for the first-order reaction rate. Since K is time-dependent, we have chosen to tabulate three of its characteristic values, i.e. K_1 , the rate at the first time channel, K_L the rate at the last time-channel (400th channel at 0.6 ns per channel), and K_{AV} , the average over 400 values corresponding to 400 time-channels. Thus K_1 shows the probability of excimer formation right after excitation. K_1 increased with pyrene concentration. This, of course, was expected since the reaction probability increases with reactant concentration. K_1 was always much larger than K_L . This is a common phenomenon with diffusion-controlled reactions in restricted geometries. It must be stressed at this point that, as can be seen from eq. (3), the difference between K_1 and K_L is larger when f is smaller. However, the relation between these two values is also influenced by the value of C_1 and (mainly) the ratio between C_1 and C_2 . It is then not surprising that even though f is here relatively large, the difference between K_1 and K_L is still large. K_1 increased upon transition to the hexagonal phase. This was done at the expense of K_L , particularly at high PD concentrations. It then means that in the H_{II} phase, the excimer-forming reaction is more localized so that long-range diffusion is not favored. Figure 1 shows that the L_α to H_{II} transition is facilitated in the presence of PD. It is then non-surprising that the phenomena observed in the H_{II} phase are more distinct at high PD concentrations. The K_{AV} values also increased with PD concentration and they became larger in the H_{II} phase. Excimer formation then is favored in the latter phase. Inspection of the values in Table 1 suggests that the higher effectiveness of the reaction in the H_{II} phase is mainly due to the large probabilities of reactant encounter at short times.

The final three columns show the values of the second-order rate constants, i.e. the probability of excimer formation per pyrene decanoate molecule. Notice again that k_1 is much larger than

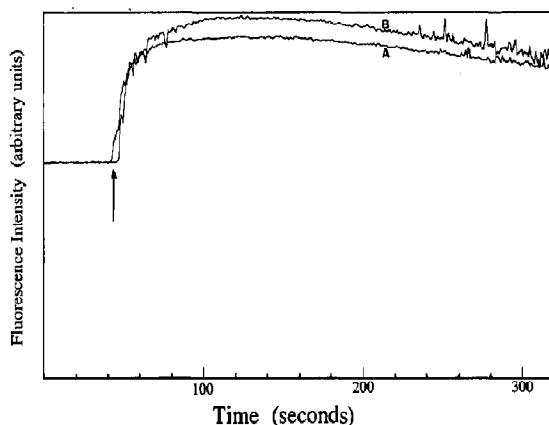


Fig. 1. Evolution of fluorescence intensity, from pH 9.5 to pH 5.0, of 2×10^{-4} M EYPE multilamellar vesicles labelled with 2×10^{-6} M NBD-PE, at 40°C, in the absence (A) and in the presence (B) of 4×10^{-5} M PD. The arrow indicates the point when 1M citric acid ($7 \mu\text{M}$ to 3 mM) was injected to lower the pH. Excitation and emission wavelengths were 470 nm and 530 nm, respectively.

K_L , showing that in the present system the probability of an encounter between an excited and an unexcited pyrene decanoate molecule decreases fast with time. This is particularly true at high PD concentration especially, in the H_{II} phase. k_1 is larger in H_{II} than in L_α as well as the overall reaction probability k_{AV} .

3. Conclusion

We have shown that a decay model containing a compilation of stretched exponentials can describe the dynamics of reactions in a lipidic environment and provides a means to calculate a time-dependent reaction rate. The values of the reaction rate give an estimate of the diffusion-controlled reaction probability at different time stages and help draw conclusions on both the structure and the dynamics of the lipidic environment. Thus in the case of L_α to H_{II} transition of EYPE at 40°C, pyrene decanoate self-quenching by excimer formation is facilitated in the hexagonal phase. The reaction is favored at short times while long-range diffusion is then less favored.

Acknowledgement

The authors gratefully acknowledge financial help from the PLATON program of scientific cooperation between Greece and France.

References

- [1] P.P. Infelta, M. Gratzel and J.K. Thomas *J. Phys. Chem.* 78 (1974) 190.
- [2] J.C. Dederen, M. van der Auweraer and F.C. de Schryver *Chem. Phys. Lett.* 68 (1979) 451.
- [3] M. Almgren, J.-E. Lofroth and J. van Stam *J. Chem. Phys.* 90 (1986) 4431.
- [4] J.M. Vanderkooi and J.B. Callis *Biochem.* 13 (1974) 4000.
- [5] J.M. Vanderkooi, S. Fischkoff, M. Andrich, F. Podo and C.S. Owen, *J. Chem. Phys.* 63 (1975) 3661.
- [6] C.S. Owen, *J. Chem. Phys.* 62 (1975) 3204.
- [7] B.M. Liu, H.C. Cheung, K.H. Chen and M.S. Habercom, *Biophys. Chem.* 12 (1980) 341.
- [8] D. Daems, M. van den Zegel, N. Boens and F.C. de Schryver, *Eur. Biophys. J.* 12 (1985) 97.
- [9] H. Lemmetyinen, M. Yliperttula, J. Mikkola, J.A. Virtanen and P.K.J. Kinnunen, *J. Phys. Chem.* 93 (1989) 7170.
- [10] G.P. L'Heureux and M. Fragata, *J. Photochem. Photobiol. B* 3 (1989) 53.
- [11] R.B. Pansu, K. Yoshimura, T. Arai and K. Tokumaru, *J. Phys. Chem.* 97 (1993) 1125.
- [12] A.K. Livesey and J.C. Brochon, *Biophys. J.* 52 (1987) 693.
- [13] D.L. Dexter, *J. Chem. Phys.* 21 (1953) 836.
- [14] A. Blumen, *Nuovo Cimento* 63B (1981) 50.
- [15] K. Allinger and A. Blumen, *J. Chem. Phys.* 72 (1980) 4608.
- [16] A. Blumen, J. Klafter and G. Zumofen, *Phys. Rev. B.* 28 (1983) 6112.
- [17] G. Zumofen and A. Blumen, *Chem. Phys. Lett.* 88 (1982) 63.
- [18] J. Klafter and A. Blumen, *J. Chem. Phys.* 80 (1984) 875.
- [19] S. Havlin and D. Ben-Avraham, *Adv. Phys.* 36 (1987) 695.
- [20] P. Lianos and G. Duportail, *Eur. Biophys. J.* 21 (1992) 29.
- [21] P. Lianos, J.C. Brochon and P. Tauc, *Chem. Phys.* 170 (1993) 235.
- [22] G. Duportail, J.C. Brochon and P. Lianos, *J. Phys. Chem.* 96 (1992) 1460.
- [23] G. Duportail and P. Lianos, *Chem. Phys. Lett.* 149 (1988) 73.
- [24] G. Duportail and P. Lianos, *Chem. Phys. Lett.* 165 (1990) 35.
- [25] G. Duportail, J.-C. Brochon and P. Lianos, *Biophys. Chem.* 45 (1993) 227.
- [26] G. Duportail, J.-C. Brochon and P. Lianos, manuscript in preparation.
- [27] P. Lianos and P. Argyrakis, *Phys. Rev. A*, 39 (1989) 4170.
- [28] P. Argyrakis, G. Duportail and P. Lianos, *J. Chem. Phys.* 95 (1991) 3808.
- [29] P. Argyrakis and R. Kopelman, *J. Phys. Chem.* 91 (1987) 2699 and 93 (1989) 225.
- [30] J.M. Seddon, *Biochim. Biophys. Acta* 1031 (1990) 1.
- [31] T.M. Allen, K. Hong and D. Papahadjopoulos, *Biochemistry* 29 (1990) 2977.
- [32] P.R. Cullis and B. de Kruijff, *Biochim. Biophys. Acta* 513 (1978) 31.
- [33] K. Hong, R.A. Baldwin, T.M. Allen and D. Papahadjopoulos, *Biochemistry* 27 (1988) 3947.
- [34] C.D. Stubbs, B.W. Williams, L.T. Boni, J.B. Hoek, T.F. Taraschi and E. Rubin, *Biochim. Biophys. Acta* 986 (1989) 89.